Telechelic Polymers between Two Impenetrable Adsorbing Surfaces

Sanjay Misra and Wayne L. Mattice*

Institute of Polymer Science, The University of Akron, Akron, Ohio 44325-3909

Received November 17, 1993; Revised Manuscript Received January 18, 1994®

ABSTRACT: This Monte Carlo study investigates telechelic chains, which can adsorb by either end to a surface. They are in an athermal solvent confined between two parallel flat plates, in a regime where the concentration in the polymer layer is at or above the overlap concentration. The chains in the adsorbed layers are not strongly perturbed compared to their free state. In other words, the chains are in the so-called "mushroom" regime. The effects of the separation of the surfaces, L, number of segments in a chain, N, and energetics of the interaction between the chain end and the surface, ϵ/kT, are explored. Of specific interest are (i) the relative populations of elastically inactive chains (free chains, dangling chains, and loops) and elastically active chains (bridges) and (ii) the structure of the adsorbed layers (*i.e.*, the total segment density distributions and the contribution of each conformation to that total). There is a well-defined threshold surface separation, L_t, corresponding roughly to twice the free layer height, $2h$, at which bridges first appear. This threshold separation appears to be independent of ϵ/kT int he semidilute regime. The fraction of chains that form bridges, f_b, can be expressed as a function of the dimensionless penetration depth $\xi/2h \approx (1 - L/L_t)$, which does not depend explicitly upon N, i.e., $f_b = f_b(\xi)$. In the dilute layer limit, the relative populations of different conformations change in the same ratio as the Boltzmann weighting factors accounting only for the energetics of end adsorption.

Introduction

The structure of the polymer layer in the vicinity of a solid–fluid interface dominates the interaction between such interfaces.[1] An adsorbed layer of polymers provides repulsive interactions between two surfaces, thus sterically stabilizing colloidal suspensions. Minute amounts of polymer added to colloidal suspensions can also cause destabilization through bridging flocculation. Addition of nonadsorbing chains to a colloidal suspension forms a depletion layer in the vicinity of a solid surface (*i.e.*, the concentration of the polymer decreases as one approaches the surface), leading to depletion flocculation. While the structure of randomly adsorbing polymers has been the subject of investigation for nearly 4 decades,[2] it is only recently that researchers have addressed the problem of tethered polymeric layers.[3] Tethered polymer layers usually refer to systems where a semidilute or concentrated layer of polymer is built at a sharp interface by attaching either one or both ends of a linear chain to a surface, while the rest of the chain, having no affinity for the surface, dangles away into the surrounding medium.

The motivation for the investigation of tethered polymer layers arises from the diverse systems in which they are found. Colloidal stabilization using singly tethered chains (attached either by chemical grafting or by adsorption of a macromolecular amphiphile) precludes bridging flocculation and leads to better colloidal stability. When dispersed in polymer blends, diblock copolymers may congregate at interfaces, forming tethered layers of both blocks in the two polymer phases.[4] Strongly segregated block copolymers form microphases where the two blocks form tethered layers at a sharp interface.[5]

Isolated tethered chains can be simulated in detail using the rotational isomeric state model[6] or the scaling approach.[7] It is, however, the dense singly tethered systems, often called brushes, that have been investigated more thoroughly in recent years using scaling ideas[7,8] and self-consistent-field theories.[9-12] Computational techniques have also been brought to bear upon the structure of polymer brushes,[13-18] as well as upon the structure of layers formed by adsorption of diblock copolymers onto surfaces,[19-21] at interfaces,[22,23] and in lamellar systems.[24,25]

A description of doubly tethered systems, formed by the adsorption of telechelic polymers or microphase separation of triblock copolymers, can be derived by an extension of techniques developed for brushes.[26-28] Bridging, which is absent in singly grafted systems, is novel to these doubly grafted systems. Thus microphase-separated triblock copolymers can form mesogels, physically cross-linked networks.[29-31] Such systems contain all of the topological features present in chemically cross-linked gels (elastically inactive loops or dangling chains, and elastically active bridges) and can serve as model systems for understanding the mechanical properties of gels.[30]

The scenario would be as interesting for telechelic polymers adsorbing on solid surfaces from solution. Suitable tailoring of the chains might alter the phase stability of a colloidal suspension, through an affect on bridging flocculation or steric stabilization. By the variation of the particle concentration (separation of the surfaces) or the degree of polymerization and polymer concentration, one might control the degree of bridging and thus change the interaction from purely repulsive to long-range atttractive. The changes in the strength of the interaction between the surface and the chelating ends, compared to the thermal energy, can control the relative populations of chains that are free, dangling ends, loops, are bridges. Indeed, one could conceivably cause reversible gelation by changing the temperature (i.e., by changing the magnitude of the thermal energy compared to the strength of the interaction between the adsorbing ends and the surface).

The objective of this study is to address some of the issues relevant to the adsorption of telechelic polymers at impenetrable surfaces, using a Monte Carlo simulation. Telechelic polymers have been chosen instead of triblock copolymers because self-assembly can introduce an additional complexity to the latter system. The surfaces in

® Abstract published in *Advance ACS Abstracts*, March 1, 1994.

0024-9297/94/2227-2058$04.50/0

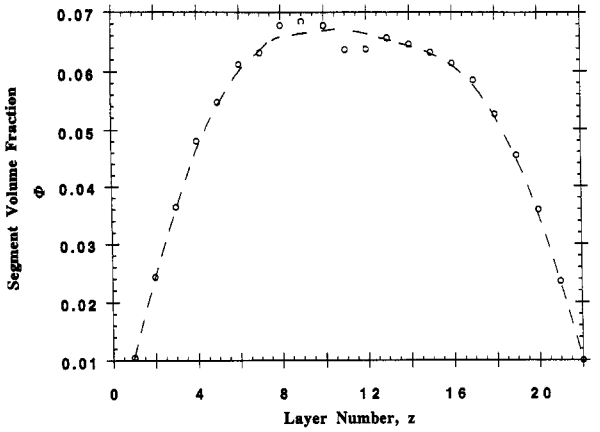

Figure 1. Profile of the density of segments for 20 chains with $N = 50$ between two nonadsorbing surfaces when $L = 21$. The points are averaged from 20 replicas equally spaced over 2×10^6 attempted moves. Continuous curves in this and other figures are meant as guides to the eye.

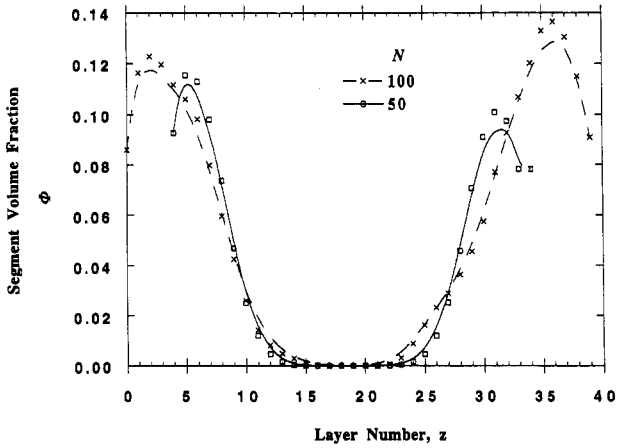

Figure 2. Density of segments for irreversible adsorption of chains with (□) $N = 50$, $L = 29$ and (×) $N = 100$, $L = 39$. The data are shifted horizontally so that $L/2$ appears midway across the figure.

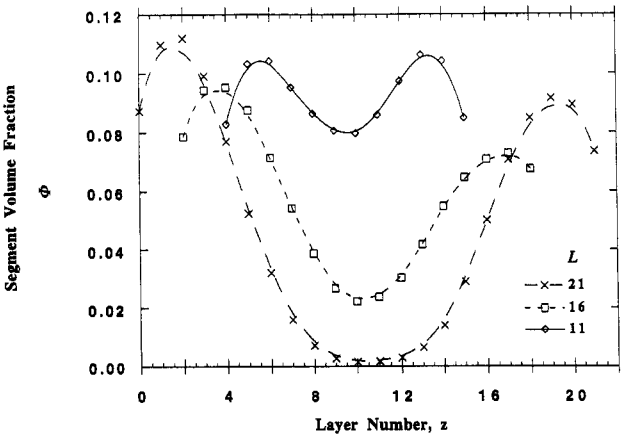

Figure 3. Density of segments for irreversible adsorption when $N = 50$ and L is (◇) 11, (□) 16, or (×) 21. The data are shifted horizontally so that $L/2$ appears midway across the figure.

this study are parallel and flat, and the solvent between them is athermal. Such a situation might occur in suspensions where the radius of gyration of the chains is much smaller than the radius of curvature of the particles. There exists an experimental probe, the surface force apparatus (SFA), that mimics just this type of a computational system. SFA has been used successfully to study the adsorption of end-functionalized chains[32] and diblock copolymers.[33] Indeed, an earlier study had focused on adsorbed triblock copolymer layers,[34] although it is only

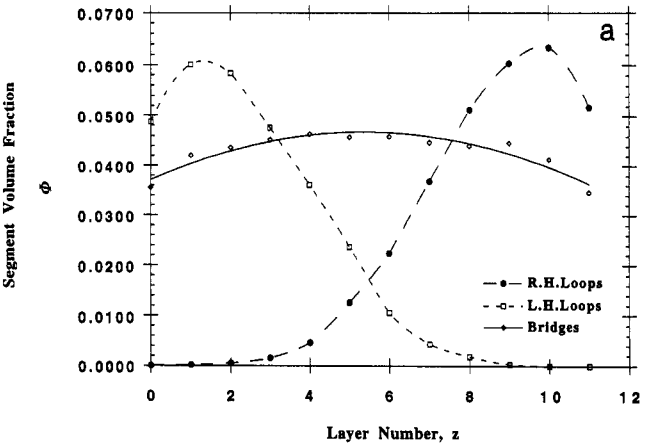

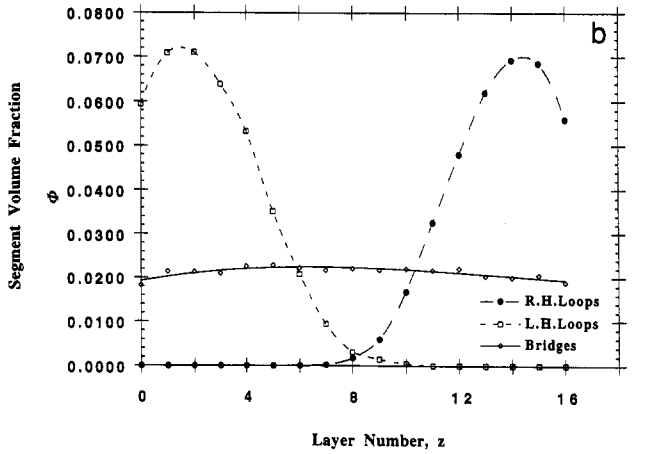

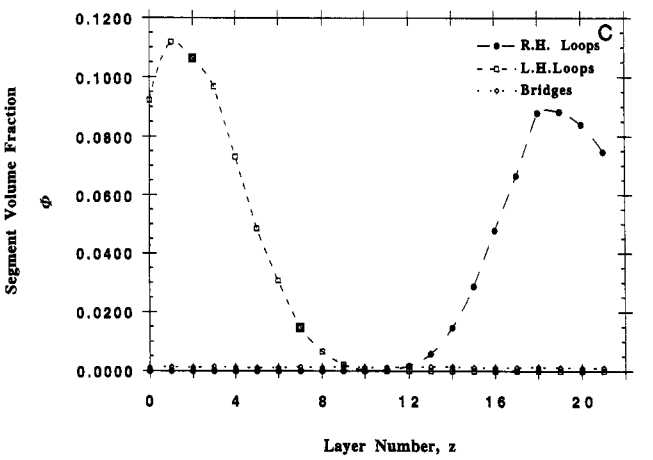

Figure 4. Contribution to the density of segments from (◇) bridges, (□) loops attached to the surface at the left, and (●) loops attached to the surface at the right in the irreversible adsorption of chains with $N = 50$ when L is (a) 11, (b) 16, and (c) 21.

recently that the SFA has been used specifically to probe bridging attraction due to telechelic polymers.[35,36]

The variable parameters in the present work are the separation of the surfaces (L), the number of segments per chain (N), and the energy of the interaction between the ends of the polymer chains and the surfaces (ϵ). Two limits of the energetics are explored. In one limit, the chain ends adsorb very strongly ($-\epsilon/kT \gg 1$), so that adsorption is irreversible. In the other limit, the adsorption energies are closer to the thermal energy ($\epsilon/kT \sim O(1)$), so that adsorption is reversible. The effect of L and ϵ/kT on the relative population of the free chains, dangling ends, loops, and bridges is explored. A simple model, valid at least in the semidilute concentration limit, that can explain the populations of various states is also introduced. The

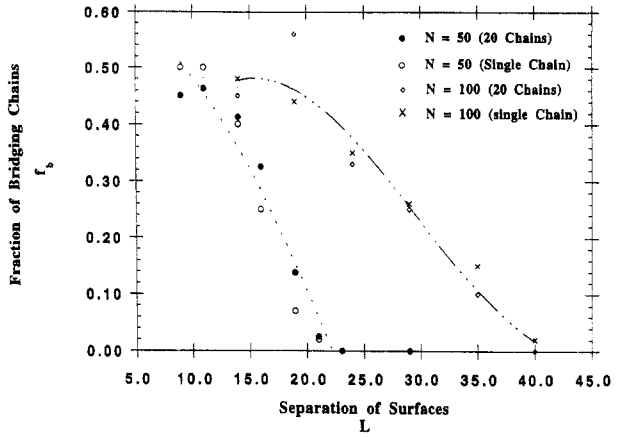

Figure 5. Dependence of f_b on L for irreversible adsorption of chains with $N = 50$ and 100.

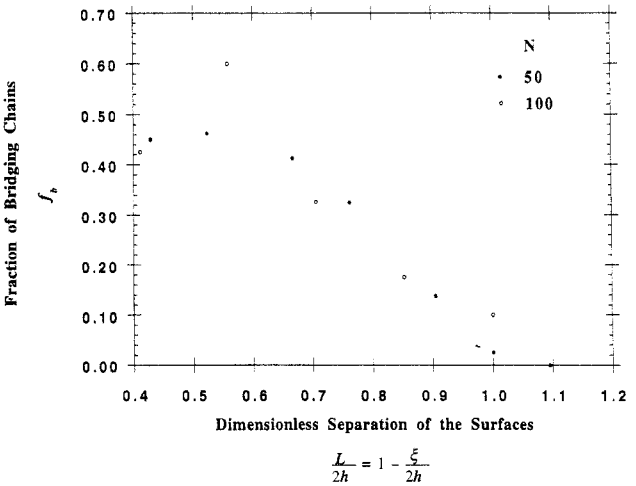

Figure 6. Dependence of f_b on the reduced separation for irreversibly adsorbed chains with $N = 50$ and 100.

structure of the tethered layers is explored through the distribution of the segment density.

The next section describes the Monte Carlo technique. Then the results are presented and discussed for their relevance for colloidal stabilization or flocculation.

Model

The Monte Carlo method was employed to study the system. A cubic lattice was used with periodic boundary conditions in the x and y directions. In a given simulation the x and y dimensions were kept at 30. There were $L + 1$ layers in the z direction. Beads in the layers at $z = 0$ and $z = L$ were considered to be adsorbed onto a surface. The number of sites accessible to a bead in the periodic box was $30^2 (L + 1)$.

The 20 chains used in the simulations give a grafting density of 0.022 ends per site. The chains were constructed as $AB_{N-2}A$. In most simulations $N = 50$, but a few simulations were performed with $N = 100$. The dimensionless root-mean-square end-to-end distances, $\langle r^2\rangle^{1/2}/l$, were 9.04 and 13.4 for chains with $N = 50$ and 100, respectively. The overlap concentrations, when estimated as $N\langle r^2\rangle^{-3/2}$, are at volume fractions of 0.068 and 0.042 respectively for $N = 50$ and 100. The value of L was chosen so that the range of average volume fractions was 0.037–0.11 for $N = 50$ and 0.056–0.148 for $N = 100$, which in most cases is larger than the estimated overlap concentration.

The initial conformations were generated as self-avoiding and mutually avoiding walks on the lattice. These conformations were relaxed without assigning any interactions between the ends of the chain and the surfaces,

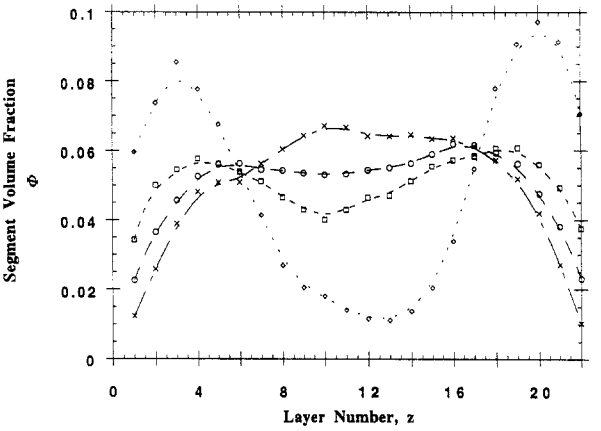

Figure 7. Density profiles for the segments of the polymer with $N = 50$ when $-\epsilon/kT$ is (×) 0, (○) 2, (□) 3, and (◇) 5.

using $2N \times 10^5$ attempted moves. The moves used were reptation, kink-jump, and crankshaft motions, which have been documented elsewhere.[37] The relaxation process cycled between a reptation move followed by moving (if possible) a randomly chosen segment using either the kink-jump or the crankshaft motion (whichever case was applicable). Moves were accepted if conditions of self-avoidance and mutual avoidance were satisfied. Figure 1 depicts a typical segment density profile for the chain with $N = 50$ after relaxation, without any end adsorption. Typical of depletion layers, the segment density decreases as one approaches the surfaces, due to entropic repulsion, and the segment density increases toward the center plane of the slit.

After the relaxation process, the energy between the chain ends and the surfaces, ϵ/kT, was turned on, and another $2N \times 10^5$ moves were attempted in order to attain equilibrium. All other pairwise interactions maintained their value of zero. The simulations followed the same procedure as during the relaxation, except that, in addition to the self-avoidance and mutual avoidance conditions, the Metropolis rule[38] was employed to determine the acceptance of a move. This rule states that, if the change in energy in an attemped move is ΔE, the move is accepted with probability

$$p = \min\{1, \exp(-\Delta E/kT)\} \quad (1)$$

All moves that do not increase the energy of the system are accepted, and those moves that increase the energy are accepted with the probability $\exp(-\Delta E/kT)$. The segment density profiles attained constant values in about $N \times 10^5$ attempted moves. The adsorption was annealed, in that the ends of a chain could translate laterally on the surfaces after adsorption. Averages were performed for ~300 replicas chosen at regular intervals over the last 3×10^6 attempted moves.

Irreversible Adsorption ($-\epsilon/kT \gg 1$). Four independently generated simulation cells, each containing 20 chains with $N = 50$, were constructed using $L = 9$, 11, 12, 16, 19, 21, 23, and 29. Three independently generated simulation cells were also constructed using 20 chains with $N = 100$ in cells with $L = 14$, 19, 24, 29, 34, and 39. Upon equilibration, each simulation box represents a topologically frozen situation because the ends of the chains are adsorbed irreversibly, leading to a system that contains only loops and bridges. At small length scales, on the order of $\langle r^2\rangle^{1/2}$, fluctuations in the density of the ends of the chains leads to unequal adsorption at the two surfaces. In order to assess the importance of chain concentration, in this weak overlap regime, we also performed simulations

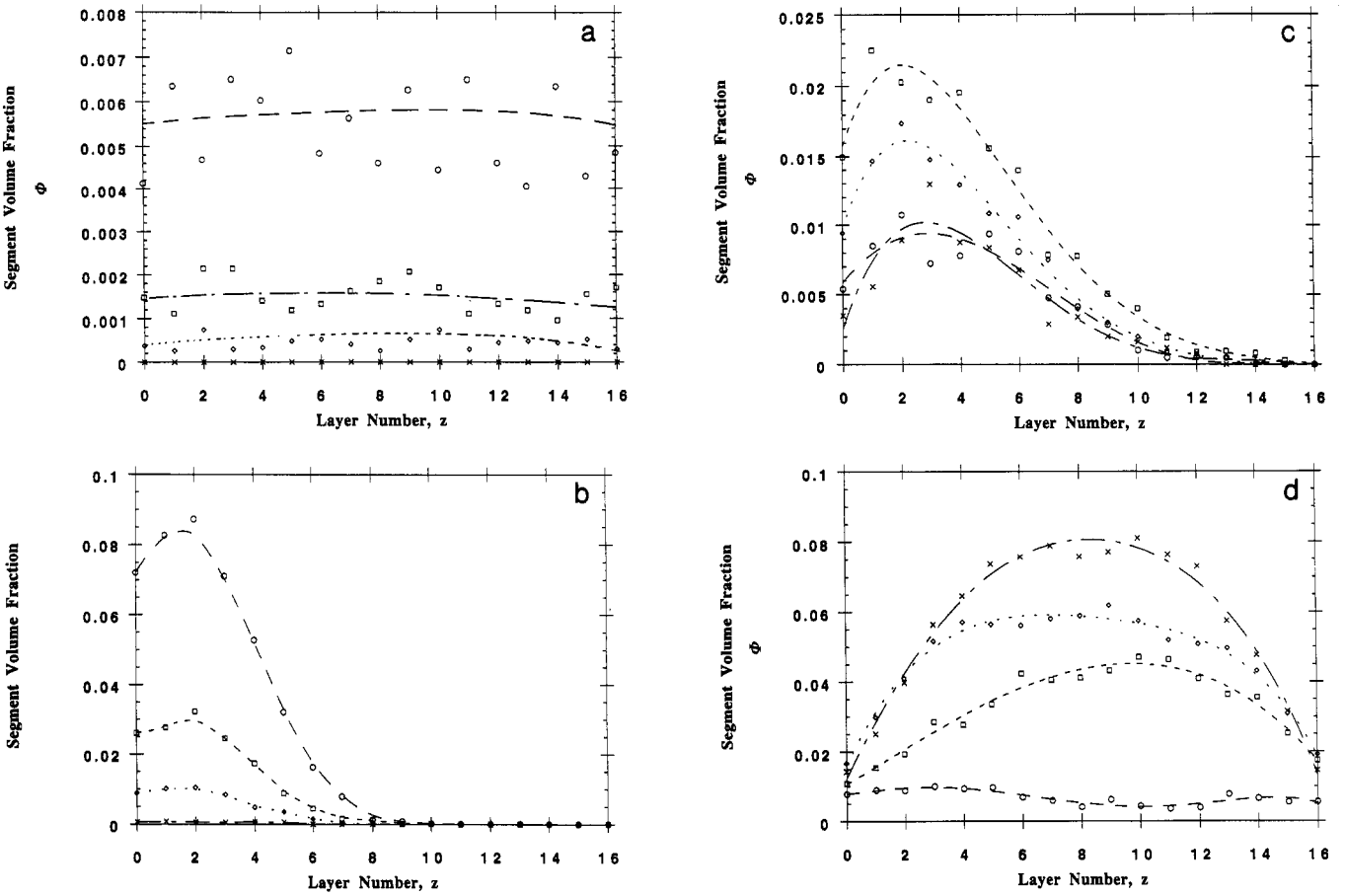

Figure 8. Density profiles for the segments in (a) bridges, (b) loops attached to the surface at the left, (c) dangling ends attached to the surface at the left, and (d) free chains of the polymer with $N = 50$ when $-\epsilon/kT$ when $-\epsilon/kT$ is (×) 1, (◇) 2, (□) 3, and (○) 5.

involving a single chain in the simulation cell. For each chain length ($N = 50$ and 100) and for each separation, 100 such simulations were performed in order to assess the bridging fraction in dilute solutions.

Reversible Adsorption ($-\epsilon/kT \sim$ O(1)). Twenty chains with $N = 50$ were placed in cells with $L = 9, 11, 14, 16, 19$, and 21 and equilibrated with binding energies, $-\epsilon$, of 1, 2, 3, and 5, in units of kT. Binding energies of polymers end functionalized with amines and polar groups on $CaCO_3$ particles have been reported to lie in this range.[39] For each L, the simulations were performed first for $-\epsilon/kT = 1$. After equilibration, the last "snapshot" was used as the starting configuration for the next larger binding energy. For each value of ϵ/kT and L, averages were performed only over one simulation cell, because the reversibility of the adsorption permits a dynamic equilibrium of the populations of the chains in different states and thus provided a larger ensemble of conformations (compared to the irreversible case, where each simulation cell corresponded to only one sample with a fixed topology).

Results and Discussion

Previous works on bridging by telechelic polymers or mesogels have focused upon the strong stretch or brush regime.[26-31] In this regime the "grafting" density of the chains is high and the chains are strongly interacting. Thus interchain interactions dominate the physics of the strong-stretch system and a mean-field approach has been used successfully to elucidate the bridging attraction. This work in contrast refers to a weakly overlapping system where intrachain interactions dominate the chain conformations. This was seen in the previous section, where the free adsorbed layer heights were shown to be of magnitude similar to that of the end-to-end distance of free chains. The results described below, thus, correspond closely to the so-called mushroom regime.

Irreversible Adsorption ($-\epsilon/kT \gg 1$). Figure 2 depicts the density of chain segments for chains with $N = 50$ and 100 when $L = 29$ and 39, respectively. These values of L are smaller than N, but they are nevertheless large enough so that bridges are not observed. All of the chains adsorb as loops instead. These profiles are typical of end-adsorbed chains, showing a steep entropic depletion near the surface followed by a maximum a short distance from the surface. The profiles then tail away gradually as the distance from the surface increases. The maximum thicknesses of the adsorbed layers are about 11 and 18 lattice units for chains with $N = 50$ and 100, respectively. These values are comparable to $\langle r^2 \rangle^{1/2}$, which suggests that the chains are not strongly stretched.

Figure 3 depicts the profiles of segments for chains with $N = 50$ at various L. Two distinct adsorbed layers are obtained at the largest L, but at the smallest L there is a strong overlap of the layers. This change in the profile of the segments of the adsorbed chains is accompanied by a change in the fraction of chains that form bridges (f_b) and loops (f_l). Parts a–c of Figure 4 depict the contributions to the density profiles from the bridges and loops. As L decreases, there is an increase in the number of bridges and in the overlap of the layers formed by the loops attached to each surface. That portion of the density profile contributed by the bridges is nearly uniform at each value of L. The contribution by the loops remains of nearly the same thickness as L changes, due to the fact that the concentration is not high enough to cause compression of opposing loops at the values of L used. There is, under this weakly overlapping regime, no dead layer, *i.e.*, a zone from which loops are excluded, unlike

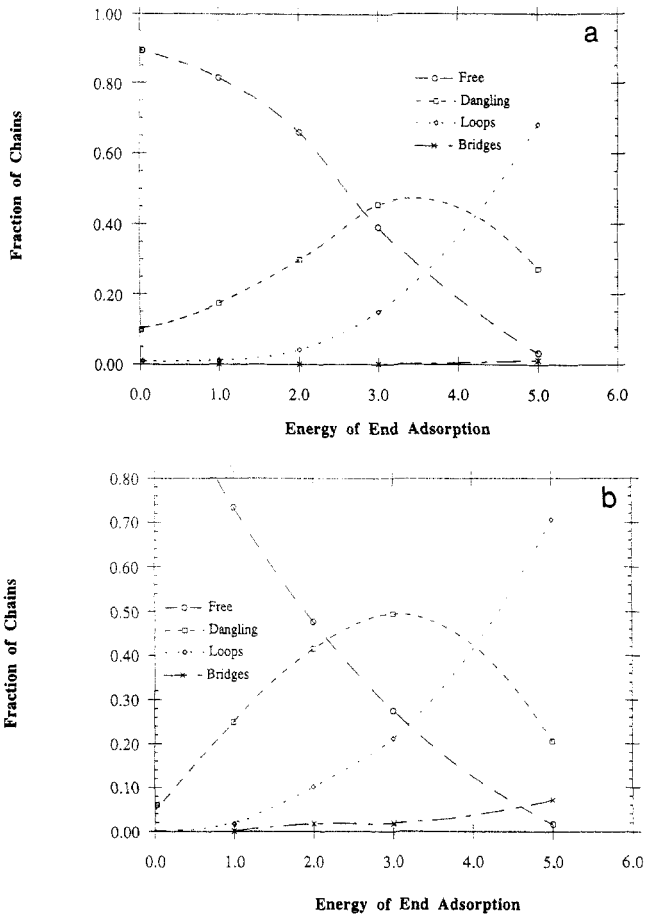

Figure 9. Fraction of the chains with $N = 50$ present as (×) bridges, (◇) loops, (□) dangling ends, and (○) free chains, as a function of $-\epsilon/kT$, when L is (a) 21 or (b) 16.

the strong-stretch regime studied for brushes[26-28] and mesogels.[29-31] Thus the penetration depth, *i.e.*, the distance by which one layer of loops penetrates into the other, is approximated by the difference between L and twice the thickness of the independent layers of loops. This information is quite useful, as will be shown below.

Figure 5 depicts the changes in f_b as L increases. Both chain lengths are investigated in this figure. Shown in the same figure are also results in the dilute limit, *i.e.*, with single chains. As expected, f_b goes to zero as L increases and attains this limit even when $L < N$, because of the entropic penalty that the chain must pay to form a bridge when L is only slightly smaller than N. The bridges vanish in Figure 5 when $L = 23$ ($N = 50$) and $L = 40$ ($N = 100$). We also expect $f_b \to 1/2$ as L becomes small. This limit is nearly reached in Figure 5 when $L = 10$ ($N = 50$) and $L = 15$ ($N = 100$). Note that there is no significant difference in bridging fractions obtained for dilute and weak overlap concentrations. Intrachain, rather than interchain, interactions thus dominate the physics.

Milner and Witten[28] recently predicted that bridging by telechelic polymers would occur when the separation of the surfaces is twice the height of a single grafted layer. Their focus was on conditions where the chains were strongly stretched. The results depicted in Figure 5 suggest that their conclusion also applies to semidilute layers assembled from short chains. Their work also yields that f_b is a scaling function of the height of a free layer, denoted by h, and the penetration thickness, denoted by ξ.

$$f_b \sim (\xi/h)^{\alpha} \qquad 2h > L \tag{2}$$

The penetration thickness is the length by which one layer of loops is penetrated by the other layer. Crudely it can be measured as $2h - L$ when $2h > L$, because the thickness of the layers formed by the loops does not change appreciably with a change in L, as shown in Figure 4. Using this definition of ξ, the data from Figure 5 is replotted in Figure 6, along with similar data obtained for chains with $N = 100$. At least for the smaller values of ξ, the results for the two different sizes of chains appear to line on a common curve. Thus, while the validity of eq 2 for brushlike conformations has been established, it could also describe the situation in semidilute layers of telechelic polymers as well. In other words, $f_b = f_b(\xi)$.

Reversible Adsorption ($-\epsilon/kT \sim$ O(1)). While irreversible adsorption might occur through a chemical reaction, often the adsorption of end-functionalized polymers occurs through a physical process (hydrogen bonding, ionic interactions involving a zwitterionic end, or physical adsorption of short anchoring blocks)[32,35,36,39] where the adsorption energy might be in the range 1–5 kT. In such a case, the system has free chains in solution and dangling chains that are adsorbed by only one end, in addition to the bridges and loops found under conditions of irreversible adsorption. Segment density profiles are depicted in Figure 7 for the chain with $N = 50$ at different values of ϵ/kT. The single maximum, observed in the middle of the slit when $\epsilon/kT = 0$, splits into two maxima as $-\epsilon/kT$ increases, and these maxima move closer to the surfaces. The separation of the segment density profile into two distinct adsorbed layers is nearly complete when $-\epsilon/kT = 5$ in Figure 7. At this energy the free chains contribute less than 10% of the density profile.

The contribution of bridges, loops, dangling chains, and free chains to the density profile when $\epsilon/kT < 0$ is depicted in the panels of Figure 8. Within the rather large fluctuations, the segments in the bridges seem to be distributed uniformly across the slit. The density profile for the loops is similar to the one observed under conditions of irreversible adsorption. The thickness of the layer produced by the loops remains constant as the adsorption becomes stronger, due to negligible interchain interchains at the concentrations employed in the simulations. The profiles for the dangling chains are typical of end-adsorbed chains and extend much further into the solution than the profiles for the loops. The free chains contribute a profile that has its maximum at the midpoint between the surfaces, as expected. The two panels of Figure 9 depict the fraction of the chains in each of the four states as a function of $-\epsilon/kT$, using two different separations for the surfaces. The concentrations of the free chains, loops, and bridges are monotonic functions of $-\epsilon/kT$, but the concentration of the dangling ends passes through a maximum at intermediate ϵ/kT. Under conditions of sufficiently strong adsorption, it becomes favorable for the dangling ends to "trade in" the freedom of their free ends by adsorbing at both ends.

A relevant question is whether the percolation threshold, *i.e.*, the separation where a finite density of bridges forms between the surfaces, changes with increasing adsorption energy. In the present system, where the layer is semidilute, the interchain interactions play a weak role in defining the conformations of the chains in the adsorbed layers. The bridging of the two surfaces should be a function solely of L and N. Thus we do not expect the percolation threshold to shift with changing adsorption energy in this semidilute regime. In the case of irreversible adsorption, the percolation threshold was $\sim 2h$ ($L \sim 23$ for $N = 50$). Figure 10 depicts the behavior of f_b as a function of L for different ϵ. If $-\epsilon/kT$ is large enough so

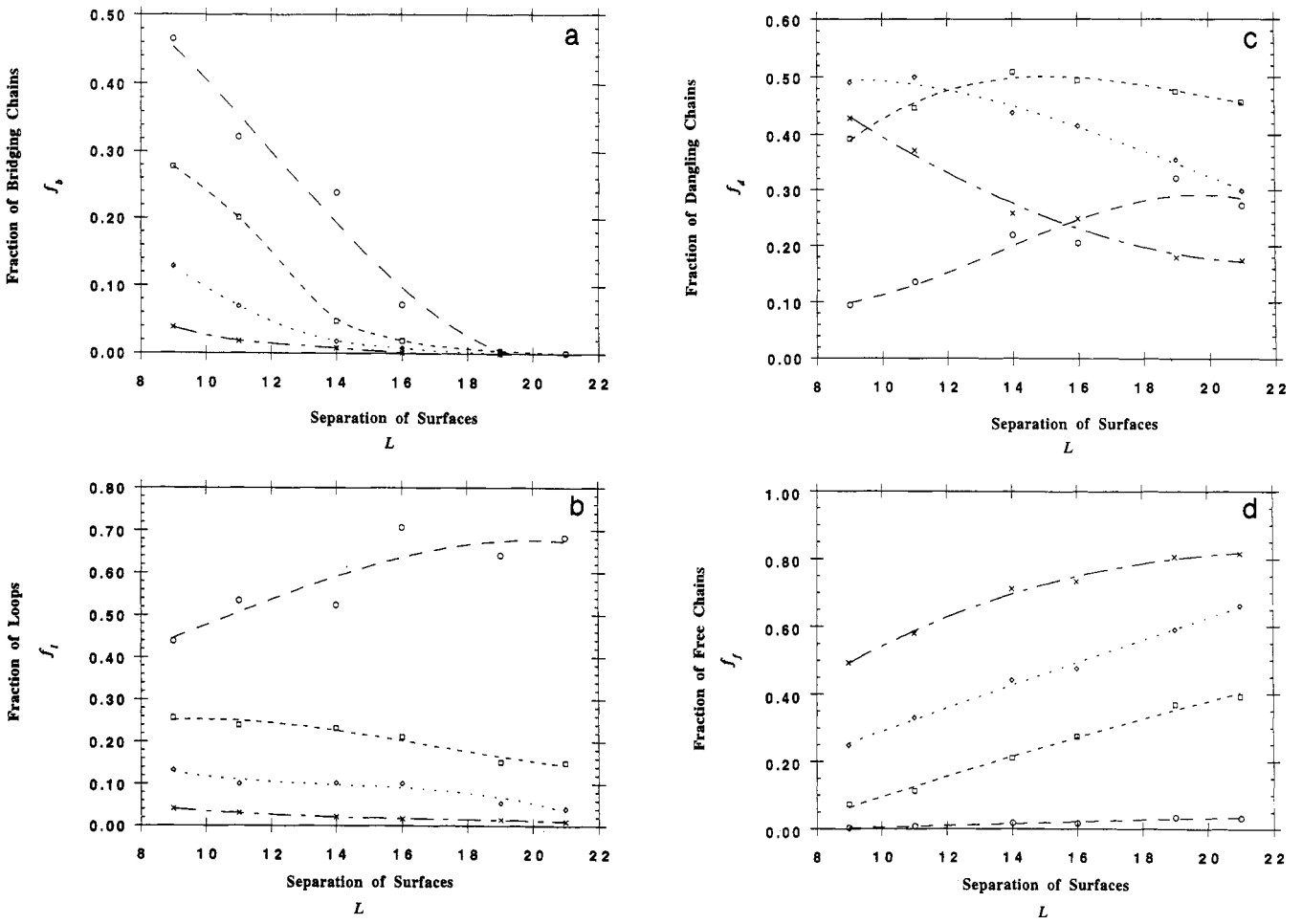

Figure 10. Fraction of the chains with $N = 50$ present as (a) bridges, (b) loops, (c) dangling ends, and (d) free chains, as a function of L, when $-\epsilon/kT$ is (×) 1, (◇) 2, (□) 3, and (○) 5.

that bridges are observed, f_b decreases as L increases and vanishes smoothly at the same threshold value of L. When the separation of the surfaces decreases from $L > N$ to $L \ll N$, some of the loops can rearrange to form bridges, which would lead to the hysteresis in force *vs* L that has been observed experimentally and attributed to this affect.[35,36] However, while there is qualitative similarity between our Monte Carlo study and the work of Dai and Toprackcioglu,[35,36] we would like to make some comment upon a few contrasting features as well. These depend upon the time scale of chain dynamics and as such are beyond the scope of this work. For a given surface separation there exists an equilibrium fraction of bridges that minimizes the free energy of the system. The work of Toprackcioglu and Dai focuses on bringing an adsorbed layer of triblock copolymers in contact with a bare surface. While repeated compression and separation lead to redistribution of the polymer upon the two surfaces, the situation does not lead to an equilibrium bridging fraction at any given separation due to the fact that on the time scale of these cycles the chains are not able to relax to an equilibrium configuration. Our Monte Carlo study corresponds to the limit where the compression–expansion cycles are performed on very large time scales, allowing for the thermal equilibration of the chains. Thus, while qualitative features of Dai and Toprackcioglu's works, *viz.*, the occurrence of bridging upon compression, are qualitatively confirmed by our simulation, we cannot comment upon the dynamic or nonequilibrium effects observed by them. Simulations in progress currently address these issues of the chain dynamics, and the results will be reported in another work.

Altering the particle concentration in a suspension would also affect the fractions of various chain populations by changing the relationship between the distance between the surfaces and the length of the chain. This process corresponds to the change in L in the present study. Parts a and d of Figure 10 examine respectively the change in the populations of bridges and free chains as functions of L. As one would expect, the population of bridges decreases monotonically with increasing L, and the population of free chains increases monotonically. The picture for dangling ends and loops is not as simple. Figure 10b depicts the fraction of chains that form loops, as a function of L. This fraction increases with increasing L for when the adsorption energy is large ($\sim 5\ kT$), largely at the expense of bridges. For lower energies, however, dangling ends compete favorably with loops due to their larger entropy, and the fraction of chains that form loops is rather insensitive to L. The fraction of chains that are dangling ends, depicted in Figure 10c, decreases montonically with increasing L at small energies ($1–2\ kT$) because the energy is not sufficient to localize the ends by adsorption, in competition with the greater entropy when the end is not so constrained. However, for larger energies the fraction of chains that are dangling ends increases with increasing L, at the expense of bridges, which have a higher stretching energy. (Note, however, that the population of dangling ends becomes smaller with increasing energy. At even higher energies the populations of dangling ends and free chains become negligible.)

In the semidilute regime, one might postulate that the fraction of chains in the ith state should be given by a Boltzmann distribution where

$$\frac{f_i}{f_f} = K_i(N,L,\Phi(\epsilon)) \exp\left(\frac{-n_i\epsilon}{kT}\right) \quad (3)$$

Here f_f is the fraction of chains that are free, K_i is a constant that takes into account entropic factors and would depend upon the type of state as well as the segment density distribution Φ (which implicitly depends upon the adsorption energy), and n_i is the number of energetic contacts that state i makes with the surface). The values of n_i are 0 for free chains, 1 for dangling chains, and 2 for loops and bridges. Since $\sum_i f_i = 1$, this postulate leads to the following expressions for the populations for the states

$$\frac{1}{f_f} = 1 + K_d(N,L,\Phi) \exp\left(\frac{-\epsilon}{kT}\right) + K_l(N,L,\Phi) \exp\left(\frac{-2\epsilon}{kT}\right) + K_b(N,L,\Phi) \exp\left(\frac{-2\epsilon}{kT}\right) \quad (4)$$

$$\frac{f_d}{f_f} = K_d(N,L,\Phi) \exp\left(\frac{-\epsilon}{kT}\right) \quad (5)$$

$$\frac{f_b}{f_f} = K_b(N,L,\Phi) \exp\left(\frac{-2\epsilon}{kT}\right) \quad (6)$$

$$\frac{f_l}{f_f} = K_l(N,L,\Phi) \exp\left(\frac{-2\epsilon}{kT}\right) \quad (7)$$

For a given separation of the surfaces, these expressions reproduce the qualitative aspects of the changes in the populations that are observed in the simulations. When $-\epsilon/kT$ is very small, f_f is on the order of unity and all of the other f_i increase as $-\epsilon/kT$ increases. With a continuing increase in $-\epsilon/kT$, eq 5 correctly predicts that f_d passes through a maximum and then decays to zero. The values of f_b and f_l approach asymptotic limits of $K_b(K_b + K_l)^{-1}$ and $K_l(K_b + K_l)^{-1}$, respectively, as $-\epsilon/kT \to \infty$.

The adsorption energy appears explicitly in the exponential term in eqs 3–7, and it also appears implicitly in K_i, through its influence on the segment density distribution. In the semidilute regime in which the simulations were performed, it is possible that the dependence of K_i on ϵ is so weak that is has little affect on the behavior of the system. This suggestion is tested by a semilog plot of the ratios of the populations of different states *vs* $-\epsilon/kT$, as is done in Figure 11. If the suggestion is valid, the plot must yield straight lines with slopes given by the difference in the number of adsorbed ends in states i and j. The data are approximated with straight lines that have slopes of about −0.05 where 0 is expected and −(0.90–0.95) where −1 is expected. This result indicates that the adsorption energy exerts its primary affect through the exponential term. In the semidilute regime covered in the simulations, the indirect influence of the adsorption energy on the prefactor can be neglected in a first approximation. This provides an independent confirmation of the results presented in Figure 5, where the bridging fraction was insensitive to interchain interactions.

Conclusions

When the adsorbed layers are semidilute, the threshold separation of the surfaces, L_t, for bridging to occur corresponds to twice the thickness of free adsorbed layers, $2h$. The threshold separation for bridging is unaffected by ϵ/kT in the semidilute regime. The fraction of chains that are bridges can be expressed as a function of the dimensionless penetration depth, $\xi/2h \approx (1 - L/L_t)$. The energy of end adsorption strongly influences the ratios of the populations of the chains in various states. In the semidilute regime, the changes in the ratios of the populations are well approximated by the ratios of Boltzmann factors that depend upon appropriate multiples of ϵ/kT.

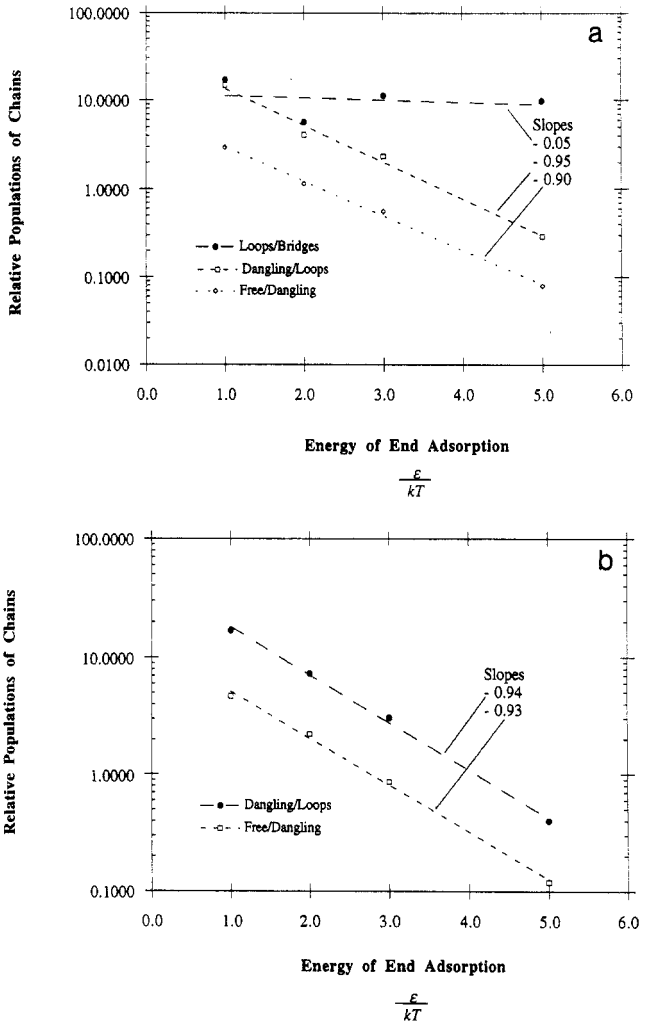

Figure 11. Logarithm of the ratio of the fraction of chains with $N = 50$ in two states, f_i/f_j, as a function of $-\epsilon/kT$, for L of (a) 16 and (b) 21.

References and Notes

(1) Napper, D. H. *Polymeric Stabilization of Colloidal Dispersions*; Academic: New York, 1983.
(2) Ploehn, H. J.; Russel, W. B. *Adv. Chem. Eng.* **1990**, *15*, 137.
(3) Halperin, A.; Tirrell, M.; Lodge, T. P. *Adv. Polym. Sci.* **1992**, *100*, 31.
(4) Feast, W. J., Munro, H. S., Eds. *Polymer Surfaces and Interfaces*; Wiley: New York, 1987.
(5) Goodman, I., Ed. *Developments in Block Copolymers-2*; Applied Science: New York, 1987.
(6) Mattice, W. L.; Napper, D. H. *Macromolecules* **1981**, *14*, 1066.
(7) de Gennes, P.-G. *Adv. Colloid Interface Sci.* **1987**, *27*, 189.
(8) Alexander, S. *J. Phys. Fr.* **1977**, *38*, 977.
(9) Cosgrove, T.; Heath, T.; van Lent, B.; Leermakers, F.; Scheutjens, J. *Macromolecules* **1987**, *20*, 1592.
(10) Skvortsov, A. M.; Gorbunov, A. A.; Pavlushkov, I. E.; Zhulina, E. B.; Borisov, O. V.; Priamitsyn, V. A. *Polym. Sci. USSR* **1988**, *30*, 1706.
(11) Milner, S.; Witten, T. A.; Cates, M. E. *Macromolecules* **1988**, *21*, 2610.
(12) Ligoure, C.; Leibler, L. *J. Phys. Fr.* **1990**, *51*, 1313.
(13) Murat, M.; Grest, G. S. *Macromolecules* **1989**, *22*, 4056.
(14) Murat, M.; Grest, G. S. In *Computer Simulation of Polymers*; Roe, R. J., Ed.; Prentice-Hall, Englewood Cliffs, NJ, 1991.
(15) Murat, M.; Grest, G. S. *Macromolecules* **1991**, *24*, 704.
(16) Binder, K.; Lai, P.-Y. *J. Chem. Phys.* **1992**, *97*, 586.
(17) Lai, P.-Y.; Zhulina, E. B. *Macromolecules* **1992**, *25*, 5201.
(18) Lai, P.-Y. *Comput. Polym. Sci.* **1992**, *2*, 157.

(19) Zhan, Y.; Mattice, W. L.; Napper, D. H. *J. Chem. Phys.* **1993**, *98*, 7502.
(20) Zhan, Y.; Mattice, W. L.; Napper, D. H. *J. Chem. Phys.* **1993**, *98*, 7508.
(21) Zhan, Y.; Mattice, W. L. *Macromolecules* **1994**, *27*, 677, 683.
(22) Wang, Y.; Mattice, W. L. *J. Chem. Phys.* **1993**, *98*, 9861.
(23) Wang, Y.; Li, Y.; Mattice, W. L. *J. Chem. Phys.* **1993**, *99*, 4068.
(24) Balaji, R.; Wang, Y.; Foster, M. D.; Mattice, W. L. *Comput. Polym. Sci.* **1993**, *3*, 15.
(25) Haliloğlu, T.; Balaji, R.; Mattice, W. L. *Macromolecules*, in press.
(26) Johner, A.; Joanny, J. F. *Europhys. Lett.* **1991**, *15*, 265.
(27) Zhulina, E. B.; Pakula, T. *Macromolecules* **1992**, *25*, 754.
(28) Milner, S. T.; Witten, T. A. *Macromolecules* **1992**, *25*, 5495.
(29) Halperin, A.; Zhulina, E. B. *Europhys. Lett.* **1991**, *16*, 337.
(30) Halperin, A.; Zhulina, E. B. *Macromolecules* **1992**, *25*, 5730.
(31) Misra, S.; Varanasi, S. *Macromolecules* **1993**, *26*, 4184.
(32) Tauton, H. J.; Toprackcioglu, C.; Klein, J. *Nature* **1988**, *333*, 712.
(33) Hadziioannou, G.; Patel, S.; Granick, S.; Tirrell, M. *J. Am. Chem. Soc.* **1986**, *108*, 2869.
(34) Patel, S.; Tirrell, M.; Hadziioannou, G. *Colloid Surf.* **1988**, *31*, 157.
(35) Dai, L.; Toprackcioglu, C. *Europhys. Lett.* **1991**, *16*, 331.
(36) Toprackcioglu, C.; Dai, L. *Macromolecules* **1992**, *26*, 6000.
(37) Binder, K. In *Computational Modeling of Polymers*; Bicerano, J., Ed.; Marcel Dekker: New York, 1992.
(38) Metropolis, N.; Rosenbluth, A. W.; Rosenbluth, M. N.; Teller, A. H.; Teller, E. *J. Chem. Phys.* **1953**, *21*, 1087.
(39) Carvalho, B. L.; Tong, P.; Huang, J. S.; Witten, T. A.; Fetters, L. J. *Macromolecules* **1993**, *26*, 4632.